

Crystal structure and electrical transport property of KMF_3 ($M = Mn, Co,$ and Ni)

S.L. Wang,¹ W.L. Li,¹ G.F. Wang,¹ D.Y. Dong,¹ J.J. Shi,¹ X.Y. Li,¹ P.G. Li,^{1,2,a)} and W.H. Tang²

¹Center for Optoelectronics Materials and Devices, Department of Physics, Zhejiang Sci-Tech University, Hangzhou, 310018, China

²School of Science, Beijing University of Posts and Telecommunications, Beijing, 100876, China

(Received 28 November 2012; accepted 30 March 2013)

The transition metal fluorides KMF_3 ($M = Mn, Co,$ and Ni) were synthesized through a simple solution route. The crystal structure, morphology and electrical transport property of the resulting products were investigated. The compound KMF_3 crystallizes in a cubic perovskite structure with space group $Pm-3m$ (No. 221). A crystal structure of KMF_3 was refined by the Rietveld method based on the X-ray powder diffraction data. The unit-cell parameters are 4.189 46(4), 4.075 58(4), and 4.025 70(2) for $KMnF_3$, $KCoF_3$ and $KNiF_3$, respectively. A metal–insulator transition was observed in temperature-dependent electrical transport characterization in the temperature range from 250 to 280 K for these three compounds, which is considered to be related to spin-exchange in this kind of material. © 2013 International Centre for Diffraction Data. [doi:10.1017/S0885715613000316]

Key words: KMF_3 , crystal structure, Rietveld method, electrical property

I. INTRODUCTION

Recently, complex perovskites fluorides have attracted considerable attention because of their various important properties, such as piezoelectric characteristics, ferromagnetic, non-magnetic insulator behavior, and photoluminescence (Alcala *et al.*, 1982; Heaton and Lin, 1982; Mortier *et al.*, 1994; Tan and Shi, 2000; Manivannan *et al.*, 2008). The typical compound KMF_3 (M : transition metal) shows that the magnetic property and spin configuration can be changed by the crystal structure itself and external conditions (Dovesi *et al.*, 1997). The cubic room temperature perovskite structure of $KMnF_3$ transforms to an orthorhombic phase at 184 K (Beckman and Knox, 1961; Kizhaev and Markova, 2011), and transition into the tetragonal phase with the space group $-P4/mbm$ at 91.5 K (Du *et al.*, 2005; Salje *et al.*, 2009). The change of structure causes a transition to uniaxial antiferromagnetism below 88.3 K (Heeger *et al.*, 1961). For the perovskite-type cobalt fluoride of $KCoF_3$, the crystal structure is slightly distorted and its spin state is changed with the temperature shift (Onishi and Yoshioka, 2007). Although the magnetic property of KMF_3 has been widely investigated, the electrical transport properties were seldom reported.

In this work, KMF_3 ($M = Mn, Co,$ and Ni) was synthesized through a simple solution route. The crystal structure of KMF_3 was refined by the Rietveld method (Rietveld, 1967) and the temperature-dependent electrical transport property was investigated.

II. EXPERIMENTAL

The complex fluorides KMF_3 ($M = Mn, Co,$ and Ni) were synthesized by the solution method from a stoichiometric

mixture of KF , $MnCl_2 \cdot 4H_2O$, $CoCl_2 \cdot 6H_2O$ and $NiCl_2 \cdot 4H_2O$. The purity of all chemical reagents is of analytical grade. For synthesis of KMF_3 , KF and MCl_2 ($M = Mn, Co,$ and Ni), were added in a 3:1 molar ratio into a water-bath along with 100 mL of deionized water. The reaction in this system may occur as follows:



The crystallographic information of prepared samples were analyzed by the powder X-ray diffraction (XRD) method using a Bruker AXS D8 DISCOVER X-ray diffractometer with $CuK\alpha$ radiation ($\lambda = 1.5406 \text{ \AA}$). The accelerating voltage and applied current were 40 kV and 40 mA, respectively. The diffraction data were collected in the $10\text{--}120^\circ 2\theta$ range by a dynamic scintillation detector using an integrated slit ($1 \times 0.6 \text{ mm}^2$ slit, 2.5° solar slit), and a $0.6 \times 0.2 \text{ mm}^2$ receiving slit, with steps of $0.02^\circ 2\theta$ and 10 s per step. The crystal structures of the synthesized products were refined by the Rietveld method using MAUD software (Lutterotti *et al.*, 1997). The morphology of the as-prepared products was characterized by field emission scanning electron microscope (FESEM, S-4800) with acceleration voltage of 5 kV. Temperature dependence of resistance was measured on the electrical transport properties measurement system (SHI-4S-1) in a four-probe configuration.

III. RESULTS AND DISCUSSION

XRD analysis was adopted to analyze the crystal structure and phase composition of synthesized products. Figure 1 shows the XRD pattern of KMF_3 ($M = Mn, Co,$ and Ni). All

^{a)} Author to whom correspondence should be addressed. Electronic mail: pgli@zstu.edu.cn

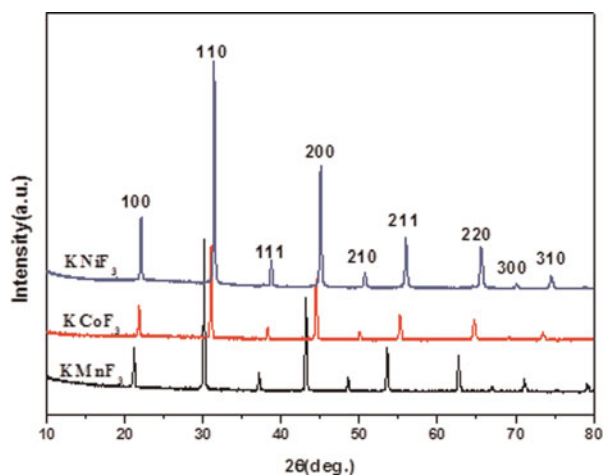


Figure 1. XRD patterns of KMnF_3 , KCoF_3 , and KNiF_3 .

the diffraction peaks in each pattern can be indexed to cubic perovskite structure KMnF_3 (PDF no. 17-0116), KCoF_3 (PDF no. 18-1006), and KNiF_3 (PDF no. 21-1002) with space group $Pm\bar{3}m$, respectively. No other diffraction peaks are detected, indicating that all the as-prepared products are pure KMF_3 . The Rietveld method was used to refine the crystal structure of KMF_3 ($M = \text{Mn}, \text{Co}, \text{and Ni}$) compound. The final values of the agreement factors were: $R_p = 3.57\%$, $R_{wp} = 4.14\%$, $R_{exp} = 3.02\%$, $R_B = 6.61\%$ for KMnF_3 , $R_p = 3.65\%$, $R_{wp} = 3.92\%$, $R_{exp} = 2.71\%$, $R_B = 7.12\%$ for KCoF_3 , and $R_p = 5.84\%$, $R_{wp} = 5.91\%$, $R_{exp} = 4.23\%$, $R_B = 8.56\%$ for KNiF_3 . Unit-cell parameters were refined to be $a = 4.18946(4) \text{ \AA}$ for KMnF_3 , $a = 4.07558(4) \text{ \AA}$ for KCoF_3 , and $a = 4.02570(2) \text{ \AA}$ for KNiF_3 . As an example of the Rietveld

TABLE I. Crystallographic data, experimental details of X-ray powder diffraction and Rietveld refinement data for KMnF_3 , KCoF_3 , and KNiF_3 .

Chemical formula	KMnF_3 , KCoF_3 , KNiF_3
Crystal system	Cubic, cubic, cubic
Space group	$Pm\bar{3}m$, $Pm\bar{3}m$, $Pm\bar{3}m$
a (Å)	4.18946(4), 4.07558(4), 4.02570(2)
Volume (Å ³)	73.531(6), 67.696(8), 65.241(5)
Z	1 1 1
d_c (g/cm ³)	3.410(3), 3.802(6), 3.939(6)
R_B (%)	6.61, 7.12, 8.56
R_p (%)	3.57, 3.65, 5.84
R_{wp} (%)	4.14, 3.92, 5.91
R_{exp} (%)	3.02, 2.71, 4.23
Diffractometer	D8 DISCOVER, Bruker AXS
Radiation type	$\text{CuK}\alpha$
Profile range ($^{\circ}2\theta$)	10–120
Step width ($^{\circ}2\theta$)	0.02

$$R_B = \frac{\sum |I_o - I_c|}{\sum I_o}, \quad R_p = \frac{\sum |Y_{io} - Y_{ic}|}{\sum Y_{io}}, \quad R_{wp} = \left\{ \frac{\sum W_i (Y_{io} - Y_{ic})^2}{\sum W_i Y_{io}^2} \right\}^{1/2},$$

$$R_{exp} = \left\{ \frac{(N - P)}{\sum W_i Y_{io}^2} \right\}^{1/2}.$$

results, the final refinement pattern of KCoF_3 was given in Figure 2. The main results of Rietveld structural refinement are presented in Table I, and the atomic parameters of KMF_3 are listed in Table II.

Figure 3 depicts the crystal structure of KMF_3 ($M = \text{Mn}, \text{Co}, \text{and Ni}$). The complex fluoride KMF_3 has a cubic perovskite structure. The center M^{2+} ion is octahedrally surrounded by fluorines. FESEM was used to observe the morphology of the synthesized complex fluorides. Figures 4(a–c) show FESEM images of KMnF_3 , KCoF_3 , and KNiF_3 , respectively.

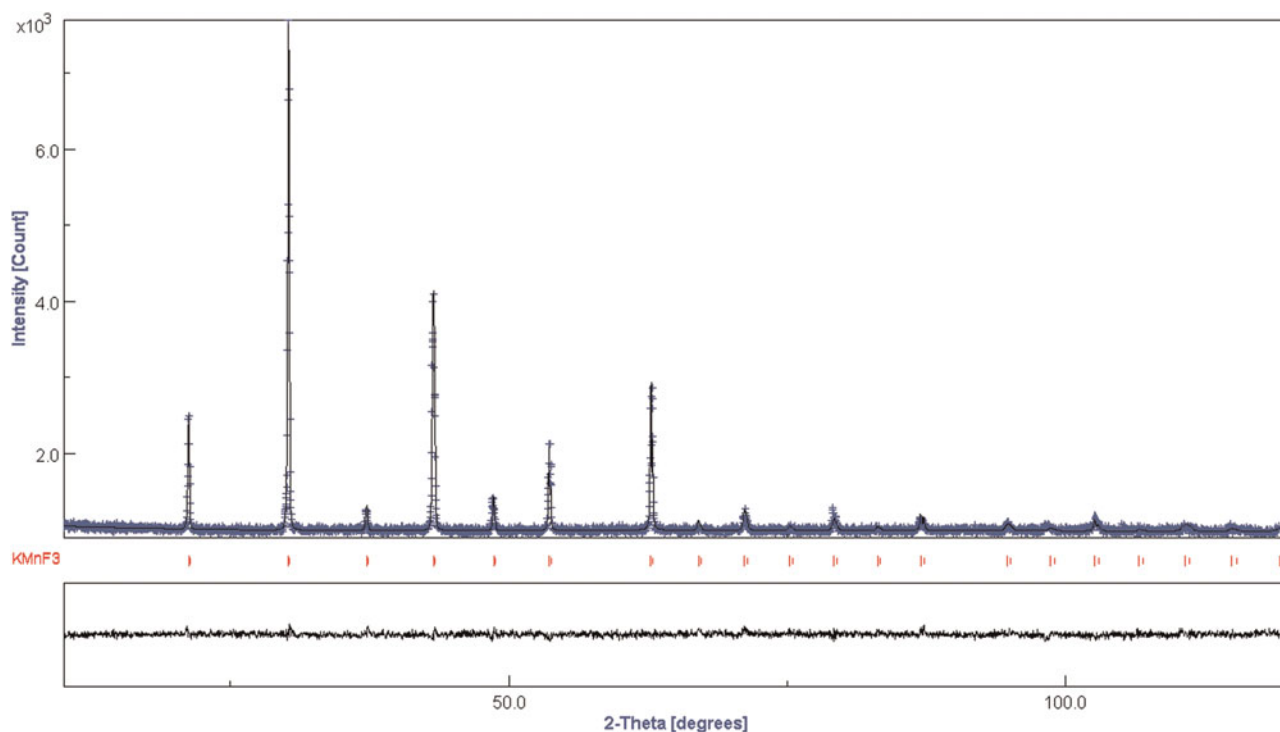


Figure 2. Final Rietveld refinement plots of the compound KMnF_3 . The small cross (+) and continuous line correspond to the experimental data and calculated pattern, respectively. The vertical bar (I) indicates the position of Bragg peaks. The bottom trace depicts the difference curve between the experimental and the calculated patterns.

TABLE II. Fractional atomic coordinates and isotropic thermal parameters for KMnF_3 , KCoF_3 , and KNiF_3 .

Atom	Site	x	y	z	Occupancy	$B_{\text{iso}} (\text{\AA}^2)$
KMnF_3						
K	1a	1/2	1/2	1/2	1	1.594
Mn	1b	0	0	0	1	-0.119
F	3c	1/2	0	0	3	2.583
KCoF_3						
K	1a	0	0	0	1	0.875
Co	1b	1/2	1/2	1/2	1	1.177
F	3c	0	1/2	1/2	3	0.398
KNiF_3						
K	1a	0	0	0	1	0.214
Ni	1b	1/2	1/2	1/2	1	1.847
F	3c	0	1/2	1/2	3	0.588

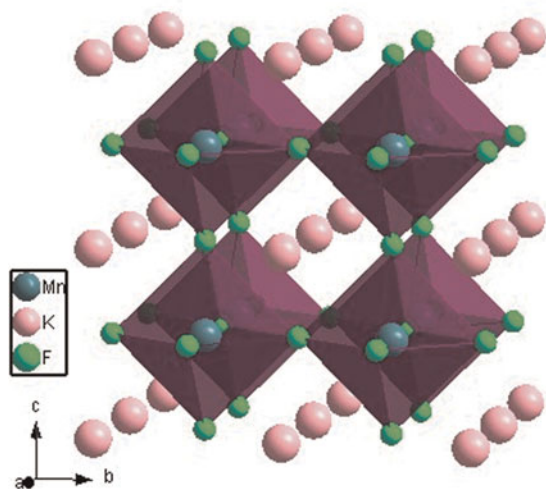


Figure 3. Crystal structure of KMF_3 ($M = \text{Mn, Co, Ni}$).

As shown in these images, the complex fluorides formed in cubic-shaped particles. These particles have regular morphology and this implies that the products are a pure and single phase.

The temperature dependence of resistance (R - T) for KMF_3 ($M = \text{Mn, Co, and Ni}$) was measured in the temperature range from 100 to 320 K (shown in Figure 5). The R - T curves of KMnF_3 , KCoF_3 , and KNiF_3 are similar. Above 262 K (275 K for KCoF_3 and 250 K for KNiF_3), the resistance of KMnF_3 decreased with the increase of temperature. Below 262 K, the resistance starts to decrease, and after a minimum value around 175 K (212 K for KCoF_3 and 160 K for KNiF_3), it eventually goes up along with decreasing temperature. It can be seen clearly that there is an abnormal transition in the temperature range from 250 K to room temperature. For these

compounds, the electron transport depends on the spin-exchange between adjacent transition metal ions significantly. Crystal parameters and magnetic properties are two important factors affecting spin-exchange. With the decrease of temperature, abnormal transitions in R - T curves should be caused by weakening of spin-exchange. For KMnF_3 , there is cubic to tetragonal transition at ~ 185 K in a single crystal, but the tetragonal short range order extends to $T > 215$ K (Salje *et al.*, 2009). For KNiF_3 , a ~ 250 K Neel temperature was reported (Nouet *et al.*, 1972; Newman, 1973). For KCoF_3 , there is a transition from cubic to tetragonal at ~ 110 K, accompanied with a magnetic transition from paramagnetic to anti-ferromagnetic (Holedn *et al.*, 1971). It is reasonable for KMnF_3 and KNiF_3 to have abnormal transition of resistance caused by crystal structure changing and magnetic phase changing, respectively. For KCoF_3 , we supposed that there was a tiny tetragonal phase existing at temperature up to ~ 275 K because of the strain in polycrystalline sample. The magnetic order is much related to the crystal phase. Not like magnetic properties, the electrical transport property is quite sensitive to local state. The sharp increase of resistance is possibly attributed to the occurrence of anti-ferromagnetic order which is related to the tetragonal phase. The upturn of resistance at low temperature is possibly because of the existence of grain boundary in KMF_3 polycrystalline compounds.

IV. CONCLUSION

KMF_3 ($M = \text{Mn, Co, and Ni}$) was synthesized through a simple solution route. The compound KMF_3 crystallizes in a cubic perovskite structure with space group $Pm-3m$. The crystal structure of KMF_3 was refined by the Rietveld method on the basis of the X-ray powder diffraction data. An abnormal electrical transport behavior was observed in the temperature range between 250 and 280 K. Such a phenomenon was

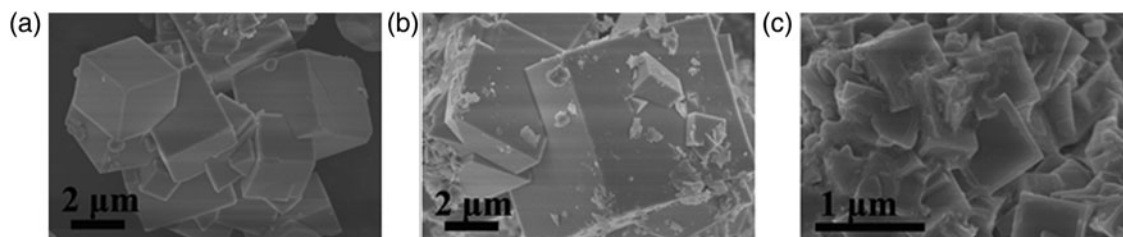


Figure 4. SEM images of KMF_3 : (a) KMnF_3 , (b) KCoF_3 , and (c) KNiF_3 .

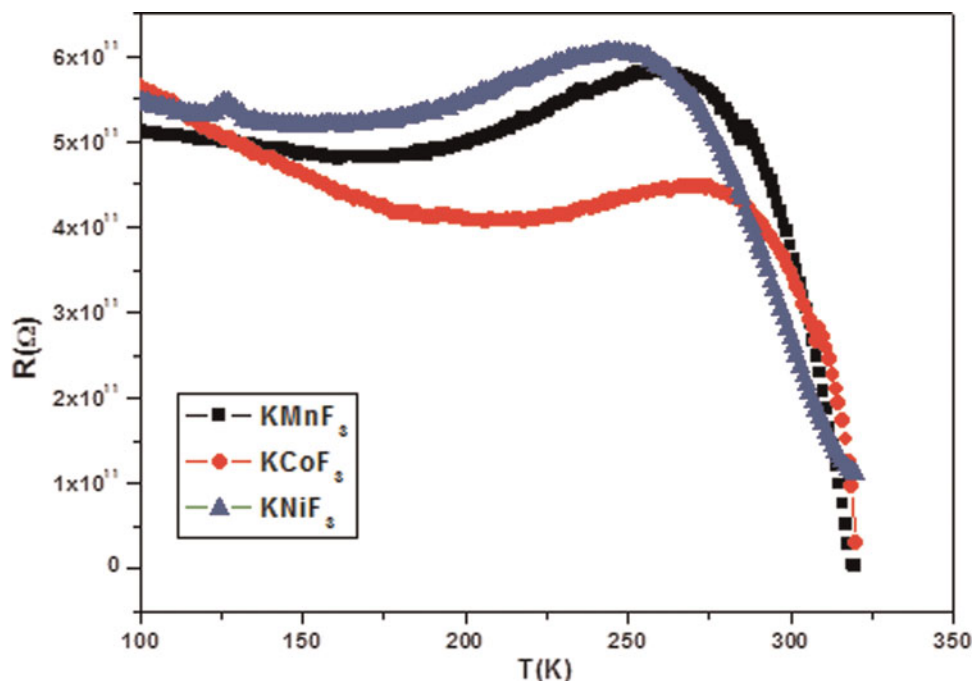


Figure 5. The temperature-dependent resistance of KMnF_3 , KCoF_3 , and KNiF_3 .

considered to be related to the spin-exchange behavior which occurred in the temperature range mentioned above.

ACKNOWLEDGEMENTS

This work was supported by the National Natural Science Foundation of China (Grant Nos. 51072182, 51172208, 51202218, 61274009, 61274017, and 61264007), Science and Technology Department of Zhejiang Province Foundation (Grant No. 2012C23037), and the Natural Science Foundation of Zhejiang Province (Grant No. Y1110519).

- Alcala, R., Sardar, D. K., and Sibley, W. A. (1982). "Optical transitions of Eu^{2+} ions in RbMgF_3 crystals," *J. Lumin.* **27**, 273–284.
- Beckman, O. and Knox, K. (1961). "Magnetic properties of KMnF_3 . I. Crystallographic studies," *Phys. Rev.* **121**, 376–380.
- Dovesi, R., Fava, F. F., Roetti, C., and Saunders, V. R. (1997). "Structural, electronic and magnetic properties of KM_3F_3 ($M = \text{Mn, Fe, Co, Ni}$)," *Faraday Discuss.* **106**, 173–187.
- Du, G. F., Zuo, J., and Yang, Q. (2005). "Simple chemical solution synthesis and photoluminescence property of KMnF_3 crystal," *Chin. J. Chem. Phys.*, **18**, 569–572.
- Heaton, R. A. and Lin, C. C. (1982). "Electronic energy-band structure of the KMgF_3 crystal," *Phys. Rev. B* **25**, 3538–3549.
- Heeger, A. J., Beckman, O., and Portis, A. M. (1961). "Magnetic properties of KMnF_3 . II. Weak ferromagnetism," *Phys. Rev.* **123**, 1652–1660.

- Holedn, T. M., Buyers, W. J. L., Svensson, E. C., Cowley, R. A., Hutchings, M. T., Hukin, D., and Stevenson, R. W. H. (1971). "Excitations in KCoF_3 -I. Experimental," *J. Phys. C: Solid State Phys.* **4**, 2127–2138.
- Kizhaev, S. A. and Markova, L. (2011). "Structural and magnetic phase transitions in KMnF_3 ," *Phys. Solid State* **53**, 1851–1854.
- Lutterotti, L., Matthies, S., Wenk, H. R., Schultz, A. J., and Richardson, J. (1997). "Texture and structure analysis of deformed limestone from neutron diffraction spectra," *J. Appl. Phys.*, **81**, 594–600.
- Manivannan, V., Parhi, P., and Kramer, J. W. (2008). "Metathesis synthesis and characterization of complex metal fluoride, KM_3F_3 ($M = \text{Mg, Zn, Mn, Ni, Cu}$ and Co) using mechanochemical activation," *Bull. Mater. Sci.*, **31**, 987–993.
- Mortier, M., Gesland, J. Y., and Rousseau, M. (1994). "Experimental and theoretical study of second-order Raman scattering in BaLiF_3 ," *Solid State Commun.* **89**, 369–371.
- Newman, D. J. (1973). "Crystal field and exchange parameters in KNiF_3 ," *J. Phys. C: Solid State Phys.*, **6**, 2203–2208.
- Nouet, J., Zarembovitch, A., Pisarev, R. V., Ferre, J., and Lecomte, M. (1972). "Determination of TN for KNiF_3 through elastic, magneto-optical, and heat capacity measurements," *Appl. Phys. Lett.* **21**, 161–163.
- Onishi, T. and Yoshioka, Y. (2007). "The theoretical study on the spin states of the perovskite-type KCoF_3 solid," *J. Surf. Sci. Nanotech.* **5**, 17–19.
- Rietveld, H. M. (1967). "Line profile of neutron powder diffraction peaks for structure refinement," *Acta. Crystallogr.* **22**, 151–152.
- Salje, E. K. H., Zhang, M., and Zhang, H. L. (2009). "Cubic-tetragonal transition in KMnF_3 : IR hard-mode spectroscopy and the temperature evolution of the (precursor) order parameter," *J. Phys. Condens. Matter*, **21**, 33–35.
- Tan, Y. W. and Shi, C. S. (2000). "Optical spectroscopy properties and charge compensation of BaLiF_3 doped with Ce^{3+} ," *J. Solid State Chem.* **150**, 178–182.